Ba-rich micas from the Yindongzi-Daxigou Pb–Zn–Ag and Fe deposits, Qinling, northwestern China

SHAO-YONG JIANG, M. R. PALMER,

Department of Geology, University of Bristol, Bristol, BS8 1RJ, UK

YAN-HE LI

Institute of Mineral Deposits, Beijing, 100037, China

AND

CHUN-JI XUE

Xi'an College of Geology, Xi'an, 710054, China

Abstract

Electron-microprobe analyses of muscovite, biotite, and feldspar are reported for the stratiform Yindongzi–Daxigou Pb–Zn–Ag and Fe deposits of Qinling, northwestern China. The micas are characterized by high Ba levels in banded albite–carbonate rocks that host the deposits. The biotite is also rich in Cl, as is biotite in the nearby Tongmugou Pb–Zn deposit, although biotite and muscovite from this deposit lack Ba enrichment. It is likely that the Ba-rich micas in the Yindongzi–Daxigou deposits formed contemporaneously from the diagenesis and/or regional metamorphism of hydrothermally altered clay minerals, with the barium being derived from entrained pore fluids that may represent relict hydrothermal fluids associated with ore deposition. During the formation of coexisting muscovite and biotite, barium is preferentially partitioned into muscovite and chloride into biotite. Together with the presence of baryte rocks in the bedded ores, these data suggest that ore deposition in the Yindongzi–Daxigou deposits took place in a more oxidising environment than in the nearby Tongmugou deposit. This difference is attributed to the contrasting sedimentary environments of the two deposits, with the Yindongzi–Daxigou deposits having formed under shallow, oxic conditions and the Tongmugou deposit under deeper, anoxic conditions.

KEYWORDS: barian muscovite, barian chlorian biotite, banded chemical rocks, Pb–Zn–Ag deposits, Fe deposit, China.

Introduction

THE chemical composition of silicate minerals associated with sediment-hosted ore deposits can provide valuable information concerning the setting and evolution of the hydrothermal systems responsible for their formation. As an example, we have recently reported the presence of Cl-rich aluminosilicate minerals within the Tongmugou Pb-Zn deposit in the Qinling mineralised belt of northwestern China (Jiang *et al.*, 1994). This study concluded that the Cl-rich minerals were the products of the alteration of volcaniclastic sedimentary rocks by saline submarine hydrothermal fluids, and that these fluids were responsible for the efficient transport of large amounts of dissolved metals as Cl-complexes to the sites of ore deposition. In this paper we extend that study to the nearby Yindongzi–Daxigou Pb–Zn–Ag and Fe deposits that also contain Cl-rich biotite, but are distinguished

Mineralogical Magazine, June 1996, Vol. 60, pp. 433–445

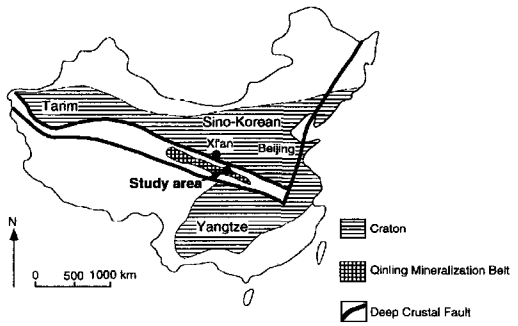

FIG. 1A. Geographic and geologic setting of the Qinling Pb-Zn mineralized belt in northwestern China.

by the additional presence of Ba-rich muscovite and biotite.

Ba-silicates such as barian-muscovite, barian-biotite, and barian-feldspar (celsian and hyalophane) have restricted parageneses. They are typically associated with stratiform Cu–Pb–Zn–Ba and Mn deposits and are believed to be related to exhalative submarine hydrothermal activity (Runnells, 1964; Deer *et al.*, 1966; Bostrom *et al.*, 1979; Fortey and Beddoe-Stephens, 1982; Coats *et al.*, 1984; Russell *et al.*, 1984; Jakobsen, 1990; Chabu and Boulegue, 1992; Fortey *et al.*, 1993). Hence, the presence of Ba-rich minerals within the Yindongzi–Daxigou deposits suggests they formed in a different sedimentary environment from the Tonmugou Pb–Zn deposit even though they are within the same mineralised belt and have a similar submarine exhalative origin (Zhang *et al.*, 1989; Zhang, 1991; Jiang *et al.*, 1994; 1995).

Geologic setting

The Qinling Pb–Zn deposits are located within Devonian (374–342 Ma) rift basins developed along a ~500 km-long E-W belt (Fig. 1A). The Yindongzi–Daxigou and Tongmugou ore deposits are located in the Shanyang-Zhashui rift basin in the eastern part of this belt (Fig.1B). A thick sedimentary sequence within this rift basin contains several sulphide and iron ore beds and associated hydrothermal sediments (siliceous and albite-rich rocks, iron carbonate and baryte rocks). The Yindongzi–Daxigou area contains several large, stratiform Pb–Zn–Ag and Fe deposits. The ore-bearing stratigraphic unit, of Middle Devonian age, is divided into two

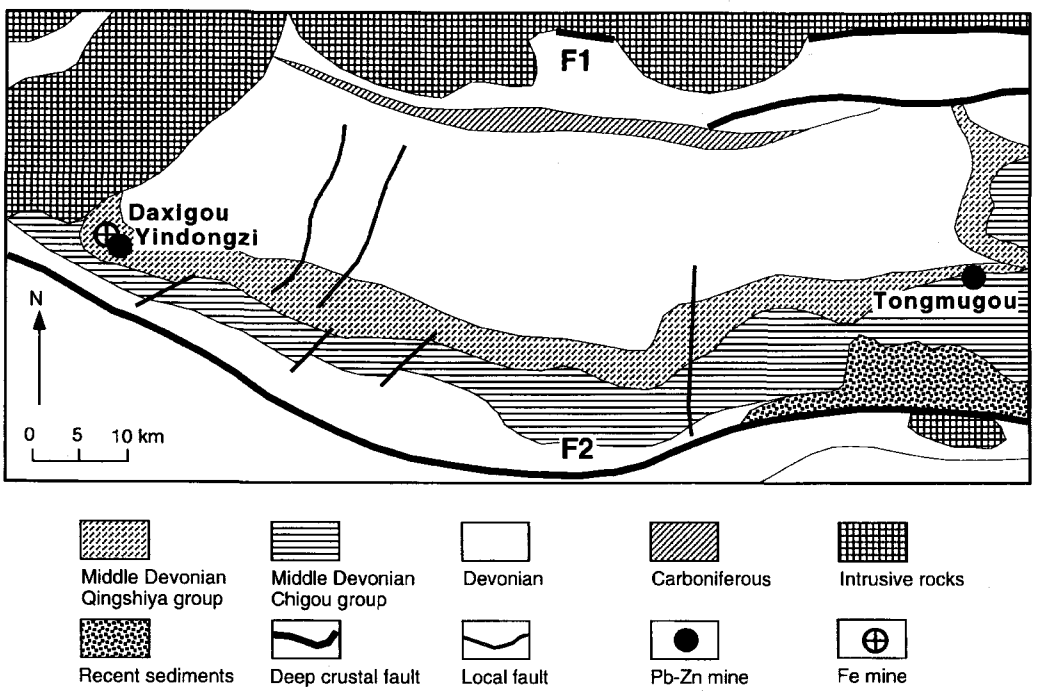

FIG. 1B. Geologic map of the eastern part of the Qinling Pb-Zn mineralized belt.

groups, known locally as the Chigou and Qingshiya Groups. The sulphide ore bodies are located in the middle to lower part of the Qingshiya Group, whereas the iron ores (mainly siderite and some magnetite) occur in the upper part. Baryte rocks are locally abundant within the banded sulphide and siderite ores. The largest sulphide orebody (No. 13) has ore grades of 2–8% Pb, 0.5–1% Zn, and 54–100g/t Ag. It is 1900 m long and has an average width of 4 m. The orebody is enriched in Cu and Ag in the lower part, and Pb and Zn in the upper part. Arsenopyrite is locally extremely abundant in the immediate footwall of the orebody. Several small galena lenses (~1 m width) and ore bands (0.5–2 cm) also occur within the host siliceous rocks and argillaceous siltstones. The magnetite–baryte–siderite and siderite orebodies, commonly several metres in width and hundreds of metres in length, occur above the sulphide orebody. Fluid inclusion studies yield homogenisation temperatures of 160–230°C for sulphide formation (Zhang *et al.*, 1989). The sulphur isotope compositions of the sulphides and sulphates in the ores range from +9 to +23 ‰ in the main orebody, with a wider range (−4 to +22 ‰) observed in the small orebodies and wallrocks. These data indicate that the sulphur was largely derived from seawater sulphate (Zhang *et al.*, 1989).

The eastern Tongmugou area contains a moderate-sized Zn–Pb deposit that occurs in the same stratigraphic unit as the Yindongzi deposit. Scapolite–biotite rocks and albite rocks are abundant in the Tongmugou deposit, but there are no finely banded siliceous rocks or baryte rocks. In addition to the massive and banded ores, some brecciated ores also exist. The breccias include albite, scapolite, and wallrock fragments within a sphalerite matrix, and are believed to be pene-contemporaneous soft-deformation structures and slump structures of syndepositional origin (Xue, 1991). The main ore belt extends 3700 m along an E–W trend, and is 0–19 m in width. The Zn ore grade is generally 1–3% and locally 3–4%. The main sulphide minerals are sphalerite, galena, and pyrite, with chalcopyrite, arsenopyrite, magnetite, pyrrhotite, and tetrahedrite as minor constituents. Tourmaline-bearing, scapolite–biotite rocks and albite rocks are intimately associated with the sulphide orebody. Later scapolite veins (with minor sphalerite and pyrite) occur near the orebody. Scapolite, biotite, and hornblende in the host rocks are Cl-rich, reflecting the saline nature of the primary hydrothermal fluids (Jiang *et al.*, 1994). The $\delta^{34}S$ values of the orebody sulphides range from +7 to +20 ‰, similar to those at Yindongzi.

Metamorphism in the Yindongzi–Daxigou and Tongmugou areas is lower greenschist facies and was associated with late Palaeozoic Hercynian deformation (Zhang, 1980). The metamorphic grade is slightly higher in the Tongmugou deposit, as shown by the presence of recrystallised, coarser grains of sulphide and gangue minerals in the orebody. This deposit is also more deformed, containing folds in the sulphide ores and associated host rocks.

Petrography and mineral chemistry

We have analysed various silicate minerals (muscovite, biotite, feldspar and chlorite) from ten host rock samples within the Yindongzi–Daxigou and Tongmugou deposits that represented different mineral assemblages, textures, and occurrences. Ba-rich micas exist within the banded chemical rocks from the Yindongzi–Daxigou, but no barium enrichment was found at Tongmugou.

Muscovite. Banded rocks composed mainly of albite, quartz, carbonates (siderite, ankerite, and dolomite), and micas (muscovite and biotite) are the main hosts of the Yindongzi–Daxigou Pb–Zn–Ag and Fe ores. Within these rocks, mica commonly occurs as a minor constituent, but is locally abundant in mica-rich beds where it forms flakes oriented parallel, or subparallel, to bedding, interbedded with siderite or ankerite beds (e.g. samples Fe-6 and Ag-39).

Sample Fe-6 is from a banded mica–albite–siderite rock, located stratigraphically between the Yindongzi Pb–Zn-Ag (sulphides) and Daxigou Fe (siderite) orebodies. Muscovite and biotite are present in two forms within this rock. They occur in fine mica-rich (up to 80 vol.%) beds in association with albite, quartz, and minor siderite, and as a minor constituent (<5 vol.%) in interbedded magnetite-bearing siderite beds (magnetite as porphyroblast). Electron microprobe analyses show that the muscovites have high Ba concentrations (up to 5.12 wt.% BaO), with FeO (4.82–5.64 wt.%) and MgO (0.85–1.45 wt.%) as the other major cations and lesser amount of SrO (0.17–0.30 wt.%) and Cl (0.01–0.11 wt.%). Cr, Ni, Ca, Na, and F were detected but their concentrations are very low or below detection levels (Table 1).

Sample Ag-39 is from a laminated albite-ankerite rock, located within strata closer to the Pb-Zn orebody than sample Fe-6. It does not contain biotite and the muscovite occurs within fine mica-albite laminations interbedded with ankerite-rich laminations. The BaO content of the muscovite ranges from 6.59 to 8.58 wt.%, higher than that of sample Fe-6, but with similar FeO, MgO, SrO, and Cl levels (Table 1).

Muscovite is also present as irregular laminae in association with pyrite in laminated albite-ankerite rocks. In sample Ag-27, near the Yindongzi Pb–Zn

TABLE 1. Representative microprobe analyses of Ba-rich muscovite from the Yindongzi-Daxigou deposits

	1	2	3	4	5	6	7	8	9	10	11
SiO_2	44.36	44.00	44.33	45.57	43.68	46.25	41.67	42.66	44.74	43.69	43.73
TiO_2	0.13	0.15	0.10	0.26	0.11	0.12	0.45	0.48	0.28	0.61	0.68
Al_2O_3	31.25	31.89	32.02	30.74	31.09	32.20	32.39	32.12	34.20	29.77	30.32
Cr_2O_3	0.00	0.03	0.05	0.01	0.00	0.00	0.42	0.07	0.00	0.12	0.11
FeO	4.82	5.44	4.59	5.64	4.89	4.82	4.16	4.74	3.15	5.53	6.10
MgO	0.95	0.97	0.85	1.15	1.45	0.98	0.64	0.79	0.62	1.01	1.10
MnO	0.03	0.00	0.00	0.01	0.02	0.00	0.03	0.00	0.00	0.09	0.00
NiO	0.02	0.00	0.02	0.06	0.00	0.00	0.00	0.03	0.00	0.00	0.02
SrO	0.17	0.30	0.23	0.21	0.21	0.00	0.22	0.12	0.00	0.16	0.23
CaO	0.03	0.03	0.04	0.07	0.05	0.05	0.03	0.04	0.00	0.01	0.02
BaO	4.21	5.04	3.77	1.49	2.28	5.12	7.95	8.77	5.45	6.59	8.58
Na_2O	0.20	0.28	0.30	0.22	0.29	0.16	0.30	0.38	0.50	0.24	0.20
K_2O	8.86	8.47	8.78	9.17	8.68	8.94	7.58	7.18	8.66	6.98	7.08
F	0.00	0.28	0.35	0.00	0.11	0.00	0.37	0.29	0.00	0.25	0.67
Cl	0.05	0.11	0.01	0.05	0.02	0.04	0.01	0.01	0.01	0.01	0.00
Total	95.07	96.99	95.44	94.64	92.88	98.67	96.22	97.68	97.60	95.06	98.84
Formulae calculated on 22 O atom anhydrous basis											
Si	6.206	6.108	6.167	6.297	6.175	6.243	5.929	5.994	6.073	6.216	6.120
Al(IV)	1.794	1.892	1.833	1.703	1.825	1.757	2.071	2.006	1.927	1.784	1.880
	8.000	8.000	8.000	8.000	8.000	8.000	8.000	8.000	8.000	8.000	8.000
AI(VI)	3.357	3.325	3.416	3.304	3.354	3.364	3.359	3.313	3.545	3.207	3.121
Ti	0.014	0.016	0.011	0.027	0.011	0.012	0.048	0.051	0.029	0.065	0.072
Cr	0.000	0.004	0.005	0.001	0.000	0.000	0.047	0.008	0.000	0.013	0.012
Fe	0.564	0.632	0.534	0.652	0.578	0.544	0.495	0.557	0.358	0.658	0.714
Mg	0.198	0.200	0.176	0.236	0.305	0.197	0.136	0.165	0.126	0.214	0.230
Mn	0.003	0.000	0.000	0.001	0.002	0.000	0.004	0.000	0.000	0.011	0.000
Ni	0.002	0.000	0.002	0.007	0.000	0.000	0.000	0.003	0.000	0.000	0.002
	4.138	4.177	4.144	4.228	4.250	4.116	4.089	4.097	4.057	4.169	4.150
Sr	0.014	0.024	0.019	0.017	0.017	0.000	0.018	0.010	0.000	0.013	0.019
Ca	0.004	0.004	0.007	0.010	0.007	0.008	0.005	0.006	0.000	0.002	0.003
Ba	0.231	0.274	0.206	0.081	0.126	0.271	0.443	0.483	0.290	0.367	0.471
Na	0.056	0.075	0.082	0.059	0.081	0.041	0.083	0.104	0.132	0.066	0.054
K	1.580	1.499	1.558	1.616	1.566	1.539	1.376	1.287	1.499	1.267	1.264
	1.884	1.877	1.871	1.782	1.797	1.858	1.924	1.889	1.921	1.715	1.810

Note: Analyses 1–6 from sample Fe-6 of banded mica-albite-siderite rock; 7–9 from sample Ag-27 of laminated albite-ankerite rock; 10–11 from sample Ag-39 of laminated albite-ankerite rock.

orebody, muscovite and pyrite laminae occur repeatedly in the albite-ankerite rocks. The laminae are parallel or subparallel to bedding with elongate aggregates that generally wrap around the albite grains, but do not cut them. Muscovite in this Ag-27 sample has the highest BaO contents measured in this study, ranging from 5.45 to 8.77 wt.%. Other element abundances are similar to those of sample Ag-39, but this sample has slightly higher Cr_2O_3 contents and lower MnO contents than sample Ag-39 (Table 1).

Examination of the muscovite structural formulae based on 22 O atoms and an anhydrous basis (Table 1) show a combination of crystal-chemical substitutions. Previous studies have shown that incorporation of Ba in the muscovite lattice can occur by one of two substitutions (Fortey and Beddoe-Stephens, 1982; Bol *et al.*, 1989; Pan and Fleet, 1991; Tracy, 1991):

$$Ba^{2+} + (Fe, Mg)^{2+} = (K, Na)^{+} + Al^{3+} \quad (1)$$

$$Ba^{2+} + Al^{3+} = (K, Na)^{+} + Si^{4+} \quad (2)$$

Reaction (1) is a combination of (2) and the common phengitic substitution of normal muscovite:

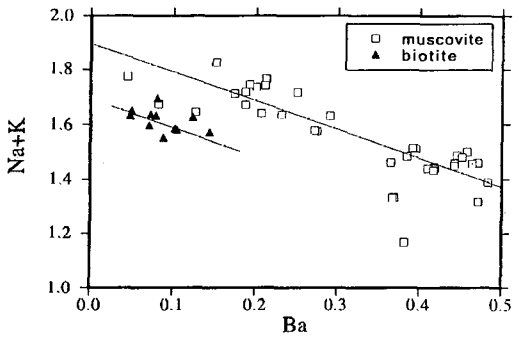

FIG. 2. Correlation of Ba with (Na+K) for muscovites and biotites from the Yindongzi-Daxigou deposits.

$$(Fe, Mg)^{2+} + Si^{4+} = (Al^{3+}_{VI}, Ti^{4+}, Cr^{3+}) + Al^{3+}_{IV} \quad (3)$$

In Yindongzi–Daxigou muscovites more than 10% of the interlayer sites are occupied by Ba (Table 1). The significant sympathetic variation of (K + Na) with Ba (Fig. 2) reflects the substitution reactions above. The well-defined negative correlation between (Mg+Fe+Si) and (Al(IV)+Al(VI)+Ti+Cr) shown in Figure 3 is due to the phengitic substitution (3). There also is a correlation between the Al(IV) and alkaline earth (Ba+Ca) contents (Fig. 4) that reflects reaction (2) and the reaction:

$$Ca^{2+} + Al^{3+} = K^{+} + Si^{4+}$$

Cr and Ti are minor, but significant, constituents in muscovite from metamorphic rocks (Heinrich and Levinson, 1955; Dymek *et al.*, 1983; Raase *et al.*, 1983; Dunn, 1984; Guidotti, 1984; Treloar, 1987). In contrast, the muscovites from the Yindongzi–Daxigou area have very low contents of Cr and Ti, and are incorporated into muscovite by the phengitic substitution reaction (3). Correlations of Ba with Cr and Ti contents are weak, and there are no obvious correlations among Ba and Fe or Mg contents (Fig. 5).

Biotite. The Ba-rich biotites analysed in this study come from the same banded mica–albite–siderite rock analysed for Ba-rich muscovites (e.g. sample Fe-3) and are closely associated with Ba-rich muscovite, albite, and siderite. The biotites have relatively high BaO contents (up to 2.21 wt.%), but these are lower than those of coexisting muscovites (Tables 1 and 2). The biotites also have high Cl (up to 1.55 wt.%), similar to biotites from the Tongmugou deposit (Jiang *et al.*, 1994). They have high FeO contents (28.30–30.97 wt.%), which are much greater than their MgO contents (3.45–5.09 wt.%). Structural formulae of the Ba- and Cl-rich biotites (Table 2) have sufficient (Si+Al) cations to completely fill the tetrahedrally-coordinated sites, in contrast to previously reported Ba- and Cl-rich biotites from other localities that have systematic deficiencies of up to 8 (Si+Al) per 22 O atoms, with the deficiencies made up by Fe (Fe^{2+} or Fe^{3+}) and possibly Zn (Guggenheim, 1984; Tracy, 1991). The Fe^{3+} contents are very low in the Yindongzi–Daxigou Ba- and Cl-rich biotites, as shown by the low total cation sums (Table 2), in contrast to the Ba- and Cl-rich biotites from the Sterling Hill Zn-deposit, New Jersey, where significant Fe^{3+} is present (Tracy, 1991).

Ba-rich biotite contains a series of exchange components (Mansker *et al.*, 1979; Tracy, 1991). For the Yindongzi–Daxigou samples, the generally sympathetic variation between Ba and (Na+K) (Fig. 2) shows that Ba is present in the interlayer sites of the biotite. A general cation correlation between Al(IV) and (Ca+Ba) is shown in Fig. 4. There is also a general correlation between Ba and Ti, but no such correlations exists among Ba and Cr,

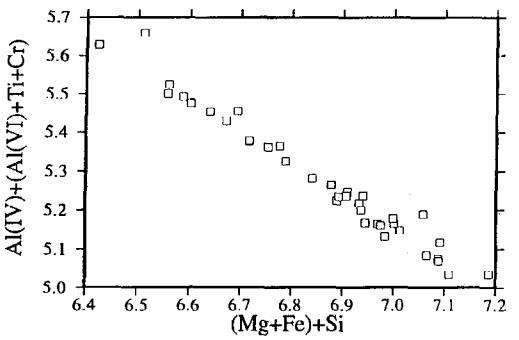

FIG. 3. Correlation of (Mg+Fe)+Si with Al(IV)+(Al(VI)+Cr+Ti) for Yindongzi-Daxigou muscovites.

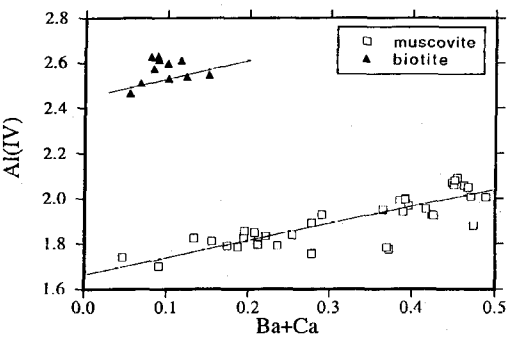

FIG. 4. Correlation of Al(IV) with (Ba+Ca) in Yindongzi-Daxigou muscovites and biotites.

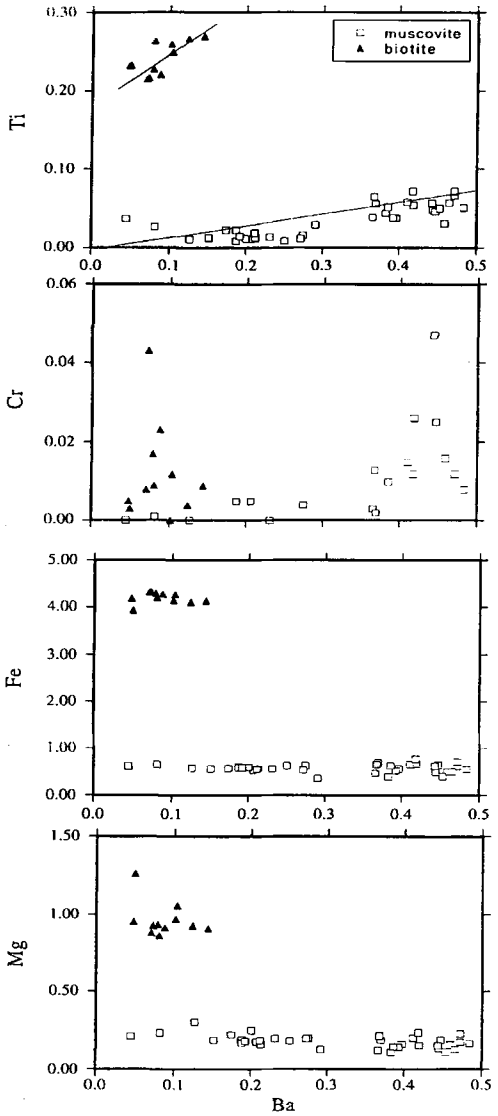

FIG. 5. Correlation of Ba with contents of Ti, Cr, Fe, and Mg in the Yindongzi-Daxigou muscovites and biotites.

Fe or Mg (Fig. 5). No correlation exists between Cl and Ba for the Yindongzi–Daxigou biotites (Fig. 6), in contrast to the biotites from Sterling Hill Zn-deposit, New Jersey (see Tracy, 1991, Fig. 8). Jiang *et al.* (1994) demonstrated that the Cl-rich biotites from the Tongmugou deposit have the predicted compositional trends of Fe-F and Mg-Cl avoidances (Munoz and Swenson, 1981; Valley *et al.*, 1982), and

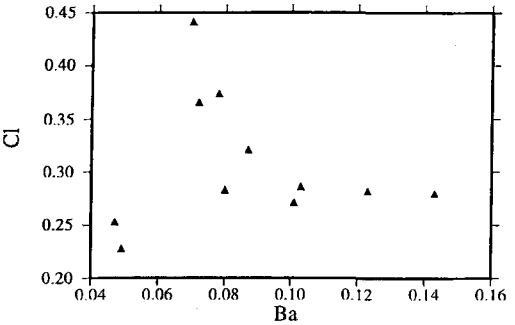

FIG. 6. Correlation of Ba and Cl for the Yindongzi-Daxigou biotites.

this also applies to the Ba- and Cl-rich biotites from the Yindongzi–Daxigou deposits (Fig. 7).

Discussion

Ba-rich muscovite has been reported from only a few metamorphic and ore-forming environments (Guggenheim, 1984; Tracy, 1991; Pan and Fleet, 1991; Chabu and Boulegue, 1992). In contrast, Ba-rich biotite and phlogopite occur widely in igneous

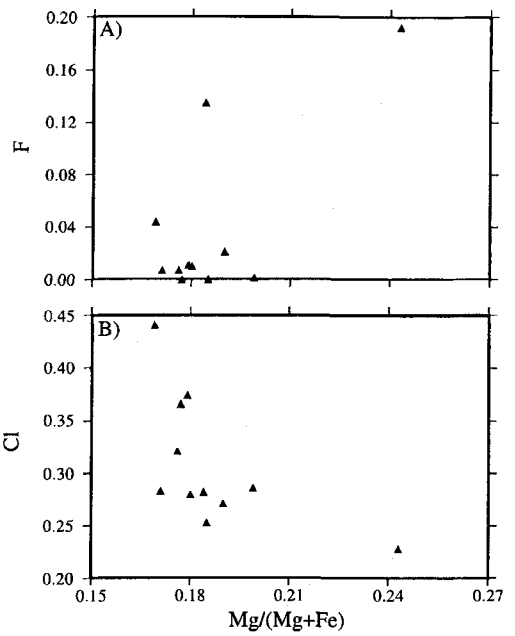

FIG. 7. Correlation of Mg/(Mg+Fe) with A) F and B) Cl for the Yindongzi-Daxigou biotites.

TABLE 2. Representative microprobe analyses of Ba- and Cl-rich biotite from the Yindongzi-Daxigou deposits

	1	2	3	4	5	6	7	8	9	10	11
SiO_2	32.34	31.75	32.35	32.93	32.18	32.10	32.69	32.42	33.45	33.03	31.95
TiO_2	1.76	1.79	2.09	2.16	1.73	1.71	2.06	2.10	1.87	1.87	1.96
Al_2O_3	15.64	15.47	15.56	15.46	15.49	15.77	15.26	15.26	15.14	15.11	14.90
Cr_2O_3	0.18	0.13	0.07	0.07	0.33	0.06	0.00	0.03	0.03	0.03	0.09
FeO	30.59	30.35	29.89	29.89	30.97	30.79	29.60	29.16	30.28	28.30	30.32
MgO	3.67	3.72	3.45	3.69	3.73	3.51	3.89	3.69	3.86	5.09	4.21
MnO	0.06	0.04	0.01	0.04	0.13	0.03	0.08	0.04	0.00	0.04	0.02
NiO	0.00	0.00	0.00	0.03	0.00	0.00	0.00	0.01	0.05	0.02	0.09
SrO	0.31	0.12	0.09	0.25	0.19	0.17	0.09	0.11	0.08	0.10	0.14
CaO	0.07	0.05	0.02	0.04	0.05	0.10	0.00	0.00	0.04	0.10	0.07
BaO	1.33	1.18	1.21	2.21	1.10	1.07	1.54	1.86	0.73	0.75	1.56
Na_2O	0.07	0.10	0.08	0.09	0.12	0.17	0.04	0.06	0.09	0.19	0.10
K_2O	7.17	7.41	7.80	7.30	7.51	7.21	7.37	7.48	7.60	7.49	7.20
F	0.01	0.02	0.01	0.02	0.00	0.08	0.04	0.25	0.00	0.37	0.00
Cl	1.14	1.30	1.00	1.00	1.29	1.55	0.95	0.99	0.90	0.81	1.00
	94.33	93.43	93.63	95.16	94.82	94.33	93.60	93.47	94.15	93.28	93.62
-O=F	0.01	0.01	0.01	0.01	0.00	0.03	0.02	0.11	0.00	0.15	0.00
-O=Cl	0.26	0.29	0.22	0.22	0.29	0.35	0.22	0.22	0.20	0.18	0.23
Total	94.07	93.13	93.40	94.93	94.53	93.94	93.37	93.14	93.94	92.95	93.39
Formulae calculated on 22 O atom anhydrous basis											
Si	5.402	5.371	5.426	5.453	5.372	5.386	5.470	5.462	5.535	5.491	5.388
Al(IV)	2.598	2.629	2.574	2.547	2.628	2.614	2.530	2.538	2.465	2.509	2.612
	8.000	8.000	8.000	8.000	8.000	8.000	8.000	8.000	8.000	8.000	8.000
Al(VI)	0.481	0.454	0.502	0.470	0.420	0.505	0.480	0.493	0.488	0.452	0.348
Ti	0.221	0.228	0.263	0.269	0.217	0.215	0.259	0.266	0.232	0.233	0.249
Cr	0.023	0.017	0.009	0.009	0.043	0.008	0.000	0.004	0.005	0.003	0.012
Fe	4.272	4.293	4.192	4.139	4.323	4.320	4.143	4.108	4.190	3.934	4.274
Mg	0.915	0.937	0.863	0.910	0.928	0.879	0.970	0.928	0.953	1.262	1.059
Mn	0.009	0.006	0.002	0.005	0.018	0.005	0.012	0.006	0.000	0.005	0.003
Ni	0.000	0.001	0.000	0.004	0.000	0.000	0.000	0.001	0.007	0.002	0.012
	5.921	5.936	5.830	5.806	5.949	5.932	5.864	5.807	5.875	5.892	5.957
Sr	0.030	0.012	0.009	0.024	0.018	0.016	0.009	0.011	0.008	0.009	0.014
Ca	0.012	0.010	0.003	0.007	0.009	0.018	0.000	0.000	0.006	0.018	0.013
Ba	0.087	0.078	0.080	0.143	0.072	0.070	0.101	0.123	0.047	0.049	0.103
Na	0.023	0.033	0.027	0.028	0.037	0.054	0.012	0.020	0.030	0.061	0.033
K	1.528	1.599	1.668	1.543	1.599	1.543	1.572	1.607	1.605	1.589	1.548
	1.680	1.732	1.786	1.745	1.735	1.702	1.694	1.761	1.696	1.726	1.711
F	0.007	0.011	0.007	0.010	0.000	0.044	0.021	0.135	0.000	0.192	0.001
Cl	0.321	0.374	0.283	0.280	0.366	0.441	0.271	0.282	0.253	0.228	0.286
	0.328	0.385	0.291	0.290	0.366	0.485	0.292	0.416	0.253	0.420	0.287

Note: Analyses 1–7 from mica-rich beds of sample Fe-6; 8–11 from siderite beds of sample Fe-6.

rocks (Wendlandt, 1977; Mansker *et al.*, 1979; Gaspar and Wyllie, 1982), metamorphic rocks (mainly calc-silicates or marbles) (Yoshii *et al.*, 1973; Bol *et al.*, 1989), and ore-related skarns (Frondel and Ito, 1968; Guggenheim, 1984; Tracy, 1991). Coexisting Ba-rich muscovite and biotite (phlogopite) has only been reported from one area in the Franklin Marble, Lime Crest (Tracy, 1991). However, significant differences exist between this occurrence and the Yindongzi–Daxigou deposits. In the Yindongzi–Daxigou deposits, Ba-rich muscovite and biotite occur in banded chemical rocks and ores of exhalative origin that are unaffected by late-stage hydrothermal veins, in contrast to the Franklin Marble locality where coexisting barian muscovite and phlogopite occur within coarse calcite-dolomite

marble at the margin of barian muscovite-albite-chromian rutile veins (Tracy, 1991). Hence, the Yindongzi–Daxigou Ba-rich micas may reflect original barium enrichment at the time of deposition of the host rocks.

The Yindongzi–Daxigou Ba-rich micas have different element distribution patterns from the Franklin Marble muscovites and phlogopites. In the Franklin Marble, Ba contents of the phlogopite (2.88–3.22 wt.% BaO) are similar or slightly higher than in coexisting muscovite (2.42–2.81 wt.% BaO), and the phlogopite has high F (2.87–3.30 wt.%) (Tracy, 1991). These barian micas formed from metamorphic vein-related fluids, so their compositional variations reflect the chemical evolution of vein fluids during mica crystallisation (Tracy, 1991). However, in the Yindongzi–Daxigou deposits, muscovite is more enriched in Ba but has less Cl than the coexisting biotite. The texture of the rocks lacks evidence that the biotite and muscovite formed at different times, but instead indicates that they formed synchronously during diagenesis and/or regional metamorphism. It appears that Ba is preferentially partitioned into the muscovite structure and Cl into biotite during their formation in the Yindongzi–Daxigou deposits. It is possible that muscovite and biotite developed from different primary clay minerals that had different patterns of Ba and Cl enrichments. However, no clay minerals have been reported with high Ba or Cl levels, hence there is no evidence for this model.

The concentrations of other elements in the Yindongzi–Daxigou Ba-rich micas are also different from those previously reported for barian micas from elsewhere. For example, barian biotite and anandite from Sterling Hill has high Mn and Zn (1.39–2.40 wt.% MnO and 4.05–9.00 wt.% ZnO, respectively) (Tracy, 1991) and barian phlogopite from Langban has even higher levels of Mn (Frondel and Ito, 1968). In contrast, the Yindongzi–Daxigou Ba-rich biotite has low Mn (0.00–0.08 wt.% MnO). Ba-rich muscovites from other localities also contain high levels of Cr, such as up to 18 wt.% Cr_2O_3 in green micas from the Archaean Malene and Isua Supergroups, and up to 3.51 wt.% Cr_2O_3 in green micas from the Franklin Marble (Dymek *et al.*, 1983; Tracy, 1991), compared with 0.00–0.42 wt.% in the Ba-rich muscovite from the Yindongzi–Daxigou deposits. These compositional differences among Ba-rich micas reflect differences in their formational environments and metamorphic histories.

In many locations Ba-rich K-feldspars occur with Ba-rich micas, such as in the stratabound Ba–Zn mineralisation in the Scottish Dalradian (Fortey and Beddoe-Stephens, 1982) and the Kipushi Zn–Pb–Cu deposit, Shaba, Zaire (Chabu and Boulegue, 1992). Ba-rich feldspars have also been reported as common constituents of silicate skarns in the Franklin Zn mine at Sterling Hill (Frondel *et al.*, 1966). However, no Ba-rich feldspar has been found at the Yindongzi–Daxigou deposits and most of the feldspar in the Yindongzi–Daxigou chemical metasediments is Ba-free albite. Some K-feldspar occurs in late metamorphic hydrothermal veins, associated with chlorite in the Yindongzi–Daxigou and Tongmugou deposits, but this feldspar is Ba-free (Table 3). The lack of Ba-rich K-feldspar production during hydrothermal-exhalative processes suggests that the hydrothermal fluids were Na-dominant and NaCl activity during ore formation was high (Jiang *et al.*, 1994; 1995).

TABLE 3. Representative microprobe analyses of albite, K-feldspar, and chlorite from the Yindongzi-Daxigou deposits

	Ag10 Ab albite	Ag11 Ab albite	Ag10K4 K-feldspar	Ag-10K5 K-feldspar	Ag10c7 chlorite	Ag10c8 chlorite	Ag27c3 chlorite	Ag39c1 chlorite	Fe6c11 chlorite
SiO_2	68.18	68.11	65.04	64.67	27.93	27.66	23.55	23.02	25.07
TiO_2	0.00	0.00	0.00	0.00	0.07	0.00	0.00	0.00	0.00
Al_2O_3	19.53	19.55	18.44	18.56	20.38	20.89	20.31	18.34	17.97
FeO	0.00	0.03	0.08	0.06	14.17	17.00	41.35	39.60	38.48
MgO	0.00	0.00	0.04	0.05	22.72	21.17	2.34	3.76	6.12
MnO	0.00	0.00	0.00	0.00	0.03	0.06	0.10	0.19	0.10
CaO	0.58	0.45	0.02	0.02	0.06	0.25	0.03	0.00	0.04
BaO	0.00	0.00	0.03	0.04	0.00	0.04	0.00	0.00	0.00
Na_2O	11.71	11.26	0.20	0.25	0.09	0.04	0.09	0.14	0.08
K_2O	0.10	0.03	16.07	16.1	0.09	0.00	0.01	0.00	0.17
F	0.00	0.00	0.00	0.00	0.26	0.31	0.00	0.00	0.00
Cl	0.00	0.00	0.00	0.00	0.02	0.02	0.01	0.00	0.17
Total	100.10	99.43	99.94	99.75	85.80	87.43	87.74	85.05	88.20

In contrast to the Ba enrichment observed in micas from the Yindongzi–Daxigou deposits, no Ba enrichment is seen in micas from the Tongmugou deposit, even though they occur in the same mineralised belt and have a common submarine exhalative origin (Zhang, 1991; Jiang *et al.*, 1994; 1995). Baryte-bearing rocks are also absent from the Tongmugou deposit, whereas at the Yindongzi–Daxigou deposits banded baryte shows a close relationship with the base-metal and iron ores. The absence of baryte and barian micas at the Tongmugou deposit suggests it formed in a different sedimentary environment from the Yindongzi–Daxigou deposits. The latter may have been located at the margin of the rift basin, a setting in which Ba enrichment has been found in many sedex-type massive sulphide deposits elsewhere. Despite the different sedimentary environments and metal associations (Zn–Pb at Tonmugou and Pb–Zn–Ag and Fe at Yindongzi–Daxigou), the ore-forming fluids at both locations were Cl-rich as indicated by their high contents of Cl in biotite.

In contrast to the Ba- and Fe-rich biotites at the Yindongzi–Daxigou deposits, those at Tongmugou are Mg-rich (Table 4). Their MgO contents range from 11.86 to 17.78 wt.%, compared with the 3.45 to 5.09 wt.% MgO in the Yindongzi–Daxigou biotites (sample Fe-6); FeO contents range from 11.38 to 17.70 wt.% in the Tongmugou biotites, compared to the 28.30 to 30.97 wt.% FeO in biotites from the Yindongzi–Daxigou deposits. Muscovite at Tongmugou also shows compositional variations that are different from those of the Yindongzi–Daxigou Ba-rich muscovite (Table 5). Sample Zn-20 from the Tongmugou albite rocks, contains muscovite with up to 1.27 wt.% Cr_2O_3 and has ragged shapes suggestive of a detrital origin. This muscovite also has low FeO contents (1.06–2.61 wt.%), compared with the higher FeO (3.15–6.34 wt.%) in the Yindongzi–Daxigou Ba-rich muscovite. In samples Zn-37 and Zn-3 from the Tongmugou biotite-scapolite rocks, muscovite in late-stage veinlets has high SiO_2 contents, suggesting they are Si-rich phengites. These muscovites are also Mg-rich with MgO>FeO, in contrast to the more Fe-rich (FeO>MgO) compositions of the barian muscovites from the Yindongzi–Daxigou deposits.

Source of the barium

Ba mobility is generally negligible during regional metamorphism (Barbey and Cuney, 1982). At the Yindongzi–Daxigou deposits, no evidence exists for a major metamorphic input of Ba into the mineralised sequence, hence the Ba in the barian micas came from within the deposit.

Baryte occurs locally in the deposits, but is not considered a likely source of Ba in the micas as no evidence exists for reaction between baryte and the barian micas, in contrast to other localities (Fortey and Beddoe-Stephens, 1982; Chabu and Boulegue, 1992). The presence of baryte generally indicates a relatively oxidising environment. During diagenetic or metamorphic events, baryte may be dissolved in a more reducing environment and the Ba released and precipitated in barian silicates (Bjorlykke and Griffin, 1973; Pan and Fleet, 1991; Tracy, 1991). However, in the Yindongzi–Daxigou area, the barian mica-bearing rocks locally contain magnetite, indicating deposition and diagenesis under relatively oxidising conditions. Baryte may be stable under reducing conditions if the environment is calcareous and alkaline (Garrels and Christ, 1965; Holland and Malinin, 1979). Under such conditions, barian silicates coexist with baryte in unmetamorphosed sedimentary rocks from central North Greenland (Jakobsen, 1990) where both minerals grew contemporaneously during diagenesis under reducing conditions, as indicated by the presence of pyrite and up to 2 wt.% organic material. Coats *et al.* (1980) considered the barian feldspars from Aberfeldy Zn–Pb–Ba deposits, Scotland, to be authigenic phases formed from a Ba–Al–Si gel with the Ba being of submarine exhalative origin (Russell *et al.*, 1984). Indeed, high Ba contents are widely associated with sediment-hosted, stratiform Zn–Pb–Ba mineralisation with the Ba originating from exhalative hydrothermal fluids (Large, 1980; Russell *et al.*, 1984).

Hence, it is likely that the source of Ba for the formation of the Yindongzi–Daxigou Ba-rich micas originates from the submarine exhalative hydrothermal fluids which were also responsible for deposition of the massive sulphide ores. These Ba- and Cl-rich hydrothermal fluids also entered the enclosing sediments as pore solutions. During diagenesis and metamorphism, these pore fluids reacted with surrounding silicate phase(s) (possibly clay minerals) to produce Ba-rich muscovites and biotites and Cl-rich biotites. The different enrichment patterns of Ba and Cl in muscovite and biotite is attributed to crystal-chemical and structural controls of the two minerals, although the mechanism is not fully understood.

Conclusions

Muscovite and biotite from the Yindongzi–Daxigou Pb–Zn–Ag and Fe deposits are enriched in Ba compared to those from the nearby Tongmugou Pb–Zn deposit. This enrichment is not the result of external Ba introduction during metamorphism, but

TABLE 4. Representative microprobe analyses of Cl-rich biotite from the Tongmugou deposit

	1	2	3	4	5	6	7	8	9
SiO_2	36.26	35.64	38.76	37.55	36.75	36.06	38.16	38.81	39.15
TiO_2	1.09	1.58	1.17	1.11	2.22	1.59	2.25	1.84	1.80
Al_2O_3	15.85	15.32	15.97	16.34	15.81	17.57	14.88	14.84	14.87
Cr_2O_3	0.14	0.14	0.06	0.07	0.14	0.02	0.15	0.08	0.01
FeO	17.05	17.70	14.76	15.77	15.42	13.90	12.38	11.66	11.38
MgO	11.86	12.03	14.17	14.22	13.91	12.83	17.20	17.78	17.16
MnO	0.12	0.14	0.05	0.06	0.07	0.16	0.03	0.15	0.11
NiO	0.00	0.00	0.03	0.01	0.03	0.00	0.00	0.00	0.04
SrO	0.09	0.13	0.20	0.25	0.24	0.16	0.25	0.12	0.36
CaO	0.04	0.52	0.08	0.07	0.05	0.14	0.05	0.08	0.03
BaO	0.00	0.00	0.00	0.00	0.00	0.18	0.08	0.44	0.24
Na_2O	0.07	0.10	0.09	0.06	0.15	0.31	0.05	0.10	0.11
K_2O	8.16	8.07	7.41	9.02	9.57	8.95	7.85	7.02	9.64
F	0.37	0.12	0.00	0.00	0.07	0.41	0.35	0.22	0.65
Cl	1.13	1.17	0.84	1.32	0.71	0.61	0.52	0.44	0.49
	92.23	92.66	93.59	95.85	95.14	92.88	94.21	93.58	96.02
-O=F	0.16	0.05	0.00	0.00	0.03	0.17	0.15	0.09	0.27
-O=Cl	0.26	0.26	0.19	0.30	0.16	0.14	0.12	0.10	0.11
Total	91.82	92.35	93.40	95.55	94.95	92.57	93.94	93.39	95.64
Formulae calculated on 22 O atom anhydrous basis									
Si	5.708	5.615	5.835	5.650	5.571	5.555	5.691	5.769	5.776
Al(IV)	2.292	2.385	2.165	2.350	2.429	2.445	2.309	2.231	2.224
	8.000	8.000	8.000	8.000	8.000	8.000	8.000	8.000	8.000
Al(Vl)	0.649	0.460	0.669	0.547	0.396	0.745	0.307	0.368	0.362
Ti	0.129	0.187	0.132	0.126	0.253	0.184	0.253	0.206	0.199
Cr	0.017	0.017	0.007	0.008	0.017	0.003	0.017	0.009	0.001
Fe	2.244	2.332	1.858	1.984	1.955	1.791	1.544	1.449	1.404
Mg	2.783	2.826	3.180	3.190	3.145	2.948	3.825	3.940	3.774
Mn	0.016	0.019	0.006	0.008	0.009	0.020	0.004	0.019	0.013
Ni	0.000	0.000	0.004	0.001	0.004	0.000	0.000	0.000	0.005
	5.839	5.841	5.857	5.864	5.779	5.691	5.950	5.992	5.758
Sr	0.008	0.012	0.017	0.022	0.021	0.014	0.022	0.011	0.030
Ca	0.007	0.088	0.013	0.011	0.008	0.023	0.009	0.013	0.005
Ba	0.000	0.000	0.000	0.000	0.000	0.011	0.005	0.026	0.014
Na	0.021	0.031	0.026	0.018	0.043	0.093	0.015	0.029	0.033
K	1.639	1.622	1.423	1.731	1.851	1.759	1.494	1.330	1.814
	1.675	1.752	1.480	1.782	1.924	1.900	1.544	1.409	1.896
F	0.184	0.060	0.000	0.000	0.032	0.198	0.163	0.105	0.304
Cl	0.301	0.312	0.214	0.337	0.183	0.159	0.131	0.110	0.123
	0.486	0.372	0.214	0.337	0.215	0.358	0.294	0.216	0.427

Note: Analyses 1–2 from sample Zn-3 of scapolite-biotite rock; 3–4 from sample Zn-37 of scapolite-biotite rock; 5–6 from sample Zn-26 of albite rock; 7–9 from sample Zn-31 of albite rock.

reflects high, original Ba concentrations in hydrothermally-derived pore fluids derived from submarine exhalative fluids. These Ba-rich pore fluids reacted with clay minerals to form Ba-rich micas during diagenesis and/or metamorphism. The presence of Ba-rich micas and abundant baryte suggests the Yindongzi–Daxigou deposits formed on the shallow oxic margins of a rift basin, whereas the Ba-poor Tongmugou deposit formed in the deeper anoxic portions of the basin. This interpretation is supported by the mineralogy of the ore deposits that exclusively comprise sulphides at

TABLE 5. Representative microprobe analyses of muscovite from the Tongmugou deposit

	1	2	3	4	5	6	7	8	9	10
SiO_2	50.26	52.31	54.79	52.14	45.22	46.08	46.46	46.27	49.69	50.84
TiO_2	0.00	0.02	0.00	0.20	0.88	0.45	0.54	0.14	0.02	0.06
Al_2O_3	26.75	28.85	28.72	25.65	24.11	31.62	32.49	34.91	32.81	34.91
Cr_2O_3	0.02	0.01	0.00	0.00	0.04	1.27	0.46	0.18	0.60	0.00
FeO	2.16	1.28	1.48	3.98	6.93	2.61	2.12	1.06	2.57	1.91
MgO	5.31	2.90	3.33	6.58	9.44	0.96	0.90	0.30	1.74	1.20
MnO	0.03	0.04	0.06	0.00	0.13	0.00	0.00	0.01	0.04	0.00
NiO	0.00	0.15	0.01	0.06	0.00	0.00	0.00	0.00	0.00	0.00
SrO	0.25	0.20	0.26	0.19	0.18	0.34	0.28	0.32	0.37	0.20
CaO	0.17	0.22	0.18	0.20	0.14	0.08	0.02	0.05	0.04	0.00
BaO	0.08	0.00	0.00	0.19	0.00	0.00	0.00	0.48	0.10	0.00
Na_2O	0.09	0.14	0.06	0.06	0.05	0.81	0.64	0.56	0.40	0.50
K_2O	8.27	9.30	7.19	8.03	6.01	9.57	9.19	9.22	7.62	7.22
F	0.00	0.40	0.25	0.00	0.00	0.14	0.60	0.00	0.00	0.23
Cl	0.01	0.00	0.01	0.03	0.01	0.04	0.03	0.03	0.03	0.01
Total	93.40	95.82	96.34	97.31	93.14	93.97	93.73	93.53	96.02	97.08
Formulae calculated on 22 O atom anhydrous basis										
Si	6.771	6.865	7.024	6.800	6.275	6.296	6.329	6.250	6.490	6.500
Al(IV)	1.229	1.135	0.976	1.200	1.725	1.704	1.671	1.750	1.510	1.500
	8.000	8.000	8.000	8.000	8.000	8.000	8.000	8.000	8.000	8.000
Al(VI)	3.018	3.328	3.364	2.742	2.217	3.387	3.545	3.807	3.541	3.761
Ti	0.000	0.002	0.000	0.020	0.092	0.046	0.055	0.014	0.001	0.006
Cr	0.002	0.001	0.000	0.000	0.004	0.137	0.050	0.019	0.062	0.000
Fe	0.243	0.140	0.159	0.434	0.804	0.298	0.241	0.120	0.281	0.204
Mg	1.066	0.567	0.636	1.279	1.953	0.196	0.183	0.060	0.338	0.229
Mn	0.003	0.004	0.007	0.000	0.015	0.000	0.000	0.002	0.004	0.000
Ni	0.000	0.016	0.001	0.006	0.000	0.000	0.000	0.000	0.000	0.000
	4.333	4.059	4.167	4.481	5.085	4.064	4.074	4.022	4.228	4.199
Sr	0.020	0.015	0.019	0.014	0.014	0.027	0.022	0.025	0.028	0.015
Ca	0.025	0.031	0.025	0.028	0.021	0.012	0.003	0.007	0.005	0.000
Ba	0.004	0.000	0.000	0.010	0.000	0.000	0.000	0.026	0.005	0.000
Na	0.024	0.036	0.015	0.015	0.013	0.215	0.169	0.147	0.102	0.123
K	1.421	1.557	1.176	1.336	1.064	1.668	1.597	1.589	1.270	1.177
	1.493	1.639	1.235	1.403	1.113	1.921	1.791	1.792	1.410	1.315

Note: Analyses 1–5 from sample Zn-37 of scapolite-biotite rock; 6–10 from sample Zn-20 of albite rock.

Tongmugou, but include Fe-carbonates, oxides, and sulphides at Yindongzi–Daxigou.

Acknowledgements

This research was supported by the Chinese National Natural Science Foundation (grant no. 49103039), the British Council, and the Royal Society. We would like to thank John Slack, Doug Robinson and an anonymous reviewer, whose helpful comments and suggestions improved this manuscript. We are also grateful to Steve Lane for his help with the electron-microprobe analyses.

References

Barbey, P. and Cuney, M. (1982) K, Rb, Sr, Ba, U, and Th geochemistry of the Lapland granulites (Fennoscandia). LILE fractionation controlling factors. *Contrib. Mineral. Petrol.*, **81**, 304–16.

Bjorlykke, K.O. and Griffin, W.L. (1973) Barium feldspar in Ordovician sediments, Oslo region, Norway. *J. Sed. Petrol.*, **43**, 461–5.

Bol, L.C.G.M., Bos, A., Sauter, P.C.C. and Jansen, J.B.H. (1989) Barium-titanium-rich phlogopites in marbles from Rogaland, southwest Norway. *Amer. Mineral.*, **74**, 439–47.

Bostrom, K., Rydell, H. and Joensuu, O. (1979) Langban — an exhalative sedimentary deposit? *Econ. Geol.*, **74**, 1002–11.

Chabu, M. and Boulegue, J. (1992) Barian feldspar and muscovite from the Kipushi Zn-Pb-Cu deposit, Shaba, Zaire. *Canad. Mineral.*, **30**, 1143–52.

Coats, J.S., Smith, C.G., Fortey, N.J., Gallagher, M.J., May, F. and McCourt, W.J. (1980) Stratabound barium-zinc mineralization in Dalradian schist near Aberfeldy, Scotland. *Trans. Inst. Mining Metall. (Sect. B: Appl. Earth Sci.)*, **89**, B110–B122.

Coats, J.S., Fortey, N.J., Gallagher, M.J. and Grout, A. (1984) Stratiform barium enrichment in the Dalradian of Scotland. *Econ. Geol.*, **79**, 1585–95.

Deer, W.A., Howie, R.A. and Zussman, J. (1966) *An Introduction to the Rock Forming Minerals.* Longman, London. 528pp.

Dunn, P.J. (1984) Barian muscovite from Franklin, New Jersey. *Mineral. Mag.*, **48**, 562–3.

Dymek, R.F., Boak, J.L. and Kerr, M.T. (1983) Green micas in the Archean Isua and Malene supracrustal rocks, southern West Greenland, and the occurrence of a barian-chromian muscovite. *Rapp. Gronlands Geol. Unders.*, **112**, 71–82.

Fortey, N.J. and Beddoe-Stephens, B. (1982) Barium silicates in stratabound Ba-Zn mineralization in the Scottish Dalradian. *Mineral. Mag.*, **46**, 63–72.

Fortey, N.J., Coats, J.S., Gallagher, M.J., Smith, C.G. and Greenwood, P.G. (1993) New stratabound barite and base metals in Middle Dalradian rocks near Braemar, northeast Scotland. *Trans. Inst. Mining Metall. (Sect. B: Appl. Earth Sci.)*, **102**, B55–B64.

Frondel, C. and Ito, J. (1968) Barium-rich phlogopite from Langban, Sweden. *Arkiv Mineralogie Geologie*, **4**, 445–7.

Frondel, C., Ito, J. and Hendricks, J.G. (1966) Barium feldspars from Franklin, New Jersey. *Amer. Mineral.*, **51**, 1388–93.

Garrels, R.M. and Christ, C.L. (1965) *Solutions, Minerals and Equilibria.* Harper, New York. 450pp.

Gaspar, J.C. and Wyllie, P.J. (1982) Barium phlogopite from the Jacupiranga carbonatite, Brazil. *Amer. Mineral.*, **67**, 997–1000.

Guggenheim, S. (1984) The brittle micas. In *Reviews in Mineralogy: Micas* (S.W. Bailey, ed.). Mineralogical Society of America, 61–104.

Guidotti, C.V. (1984) Micas in metamorphic rocks. In *Reviews in Mineralogy: Micas* (S.W. Bailey, ed.). Mineralogical Society of America, 357–467.

Heinrich, E.W. and Levinson, A.A. (1955) Studies in the mica group; X-ray data on roscoelite and barium-muscovite. *Amer. J. Sci.*, **253**, 39–43.

Holland, H.D. and Malinin, S.D. (1979) The solubility and occurrence of non-ore minerals. In *Geochemistry of Hydrothermal Ore Deposits* (2nd edition) (H.L. Barnes, ed.). John Wiley and Sons, Inc., 461–501.

Jakobsen, U.H. (1990) A hydrated barium silicate in unmetamorphosed sedimentary rocks of central North Greenland. *Mineral. Mag.*, **54**, 81–9.

Jiang, S.-Y., Palmer, M.R., Xue, C.J. and Li, Y.H. (1994) Halogen-rich scapolite-biotite rocks from the Tongmugou Pb-Zn deposit, Qinling, northwestern China: Implications for the ore-forming processes. *Mineral. Mag.*, **58**, 543–52.

Jiang, S.-Y., Palmer, M.R., Li, Y.-H. and Xue, C.-J. (1995) Chemical compositions of tourmaline in the Yidongzi-Tongmugou Pb-Zn deposits, Qinling, China: Implications for the hydrothermal ore-forming processes. *Mineral. Deposita*, **30**, 225–34.

Large, D.E. (1980) Geological parameters associated with sediment-hosted submarine exhalative Pb-Zn deposits: An empirical model for mineral exploration. *Geol. Jahrb.*, **40**, 59–129.

Mansker, W.L., Ewing, R.C. and Keil, K. (1979) Barian-titanian biotites in nephelinites from Oahu, Hawaii. *Amer. Mineral.*, **64**, 156–9.

Munoz, J.L. and Swenson, A. (1981) Chloride-hydroxyl exchange in biotite and estimation of relative HCl/HF activities in hydrothermal fluids. *Econ. Geol.*, **76**, 2212–21.

Pan, Y. and Fleet, M.E. (1991) Barian feldspar and barian-chromian muscovite from the Hemlo area, Ontario. *Canad. Mineral.*, **29**, 481–98.

Raase, P., Raith, M., Ackermand, D., Viswanathan, M.N. and Lal, R.K. (1983) Mineralogy of chromiferous quartzites from south India. *J. Geol. Soc. India.*, **24**, 502–21.

Runnells, D.D. (1964) Cymrite in a copper deposit, Brooks Range, Alaska. *Amer. Mineral.*, **49**, 158–65.

Russell, M.J., Hall, A.J., Willan, R.C.R., Allison, I., Anderton, R. and Bowes, G. (1984) On the origin of the Aberfeldy celsian+baryte+base-metal deposits, Scotland. *Symposium on prospecting in areas of glaciated terrain, Glasgow, Scotland.* 158–70.

Tracy, R.J. (1991) Ba-rich micas from the Franklin Marble, Lime Crest and Sterling Hill, New Jersey. *Amer. Mineral.*, **76**, 1683–93.

Treloar, P.J. (1987) Chromian muscovites and epidotes from Outokumpu, Finland. *Mineral. Mag.*, **51**, 593–9.

Valley, J.W., Peterson, E.U., Essene, E.J. and Bowman, J.R. (1982) Fluorphlogopite and fluortremolite in Adirondack marbles and calculated C-O-H-F fluid composition. *Amer. Mineral.*, **67**, 545–57.

Wendlandt, R.F. (1977) Barium-phlogopite from Haystack Butte, Highwood Mountains, Montana. In *Carnegie Inst. of Washington Year Book 1977*, 534–9.

Xue C. (1991) A study on the seafloor hydrothermal sedimentary nature of jasperoid rocks in Yindongzi. *Mineral. Petrol.*, **11**, 31–40 (in Chinese).

Yoshii, M., Maeda, K., Kato, T., Watanabe, T., Yui, S., Kato, A. and Nagashima, K. (1973) Kinoshitalite, a new mineral from the Noda-Tamagawa mine, Iwate

Prefecture. *Chigaku Kenkyu*, **24**, 181–90.

Zhang B.Y., Chen, D.X., Li, Z.J. and Gu, X.M. (1989) *The regional geochemistry of the Zhashui-Shanyang sulfide mineralization zone, Shaixi, China.* Chinese Geol. Univ. Pub. House, Beijing, 249 pp. (in Chinese).

Zhang, F. (1991) Exhalites associated with Pb-Zn mineralization in Devonian system and their prospecting implications, Qinling, China. *Chinese J. Geochem.*, **10**, 348–56.

Zhang, Q.S. (1980) *Metamorphic geology of east Qinling*. People's Pub. House, Jilin. 215 pp. (in Chinese).

[*Manuscript received 27 February 1995: revised 3 May 1995*]